Available Power Gain, Noise Figure, and Noise Measure of Two-Ports and Their Graphical Representations

H. FUKUI

Abstract—The expressions for available power gain and noise measure of linear two-ports are introduced in terms of the two-port parameters and the gain and the noise parameters, respectively. Their graphical representations on the source admittance plane with rectangular coordinates are also shown. Furthermore, it is shown that the behavior of available power gain, noise figure, and noise measure can be represented on the Smith-chart or the complex reflection coefficient plane of the source admittance. It is more convenient to investigate the gain and noise performance of amplifiers over a wide range of source admittance in this representation than with rectangular coordinates. As an example of the graphical representation the gain and noise performance of a microwave transistor is illustrated on the Smith-chart.

I. Introduction

IT IS WELL KNOWN that the noise figure of linear twoports is a function of the source admittance [1]. The noise figure of a linear two-port driven by a signal source with an admittance, $Y_s = G_s + jB_s$, can be expressed as

$$F = F_{\min} + \frac{R_{ef}}{G_s}\{(G_s - G_{of})^2 + (B_s - B_{of})^2\} \quad (1)$$

where $F_{\min}$ is the minimum noise figure, R_{ef} is a parameter with units of resistance, and G_{of} and B_{of} are the particular source conductance and susceptance, respectively, which produce $F_{\min}$. Thus, the noise figure characteristics of linear two-ports can be completely described by the four noise parameters, $F_{\min}$, R_{ef}, G_{of}, and B_{of}. Furthermore, a graphical representation of the noise figure on a rectangular coordinate system of source admittance has been given by Rothe and Dahlke [2].

In recent years, the noise measure has been proposed by Haus and Adler [3] as a more significant parameter than the noise figure when considering cascaded two-ports. The noise measure M is defined as [4]

$$M = \frac{F - 1}{1 - \frac{1}{G_a}} \quad (2)$$

where G_a is the available power gain of the two-port.

Since G_a and F are functions of source admittance Y_s, M will also be a function of Y_s. However, this situation has not previously been made clear. This paper will consider the problem and show that constant-M loci can be mapped in the source admittance plane. Another purpose of this paper is to demonstrate how the constant G_a, F, and M loci appear on the Smith-chart representation.

Manuscript received April 19, 1965; revised November 3, 1965.
The author is with Bell Telephone Laboratories, Inc., Murray Hill, N. J.

II. Available Power Gain

A. The Available Power Gain of Two-ports

The available power gain G_a of the two-port shown in Fig. 1 is defined as the ratio of the available power at

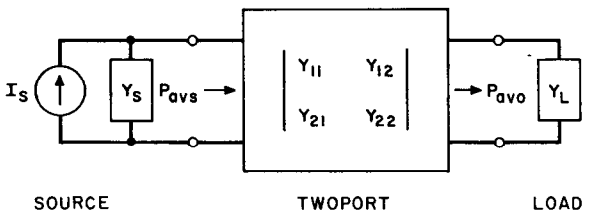

Fig. 1. Available power gain of a twoport.

the output P_{avo} to the available power from the source P_{avs}, i.e.,

$$G_a = \frac{P_{avo}}{P_{avs}}. \quad (3)$$

G_a is a function of the two-port parameters, such as y-parameters, and the source admittance Y_s.

Using the same procedure given by Linvill and Gibbons [5], G_a is expressed as follows.

$$G_a = \frac{|y_{21}|^2 G_s}{g_{22}|y_{11} + Y_s|^2 - Re\,[y_{12}y_{21}(y_{11} + Y_s)^*]}. \quad (4)$$

B. Alternate Expression for Available Power Gain

From the expression for G_a its maximum value, $G_{a_{max}}$, is derived for the particular source admittance $Y_{og} = G_{og} + jB_{og}$ as follows.

$$G_{a_{max}} = \left|\frac{y_{21}}{y_{12}}\right| \frac{1}{k + \sqrt{k^2 - 1}} \quad (5)$$

$$G_{og} = \frac{|y_{12}y_{21}|}{2g_{22}}\sqrt{k^2 - 1} \quad (6)$$

$$B_{og} = -b_{11} + \frac{Im\,(y_{12}y_{21})}{2g_{22}} \quad (7)$$

where

$$k = \frac{2g_{11}g_{22} - Re\,(y_{12}y_{21})}{|y_{12}y_{21}|}. \quad (8)$$

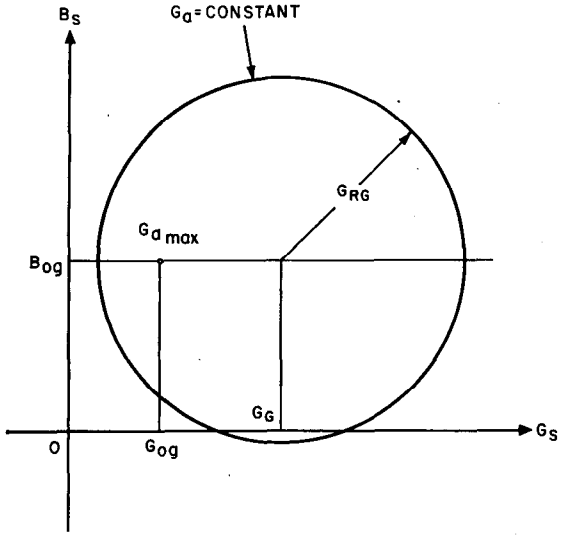

Fig. 2. Constant available power gain locus on rectangular source admittance plane.

Now (4) is rewritten using a set of gain parameters, $G_{a_{max}}$, G_{og}, B_{og}, and a parameter R_{eg}:

$$\frac{1}{G_a} = \frac{1}{G_{a_{max}}} + \frac{R_{eg}}{G_s}[(G_s - G_{og})^2 + (B_s - B_{og})^2] \tag{9}$$

where

$$R_{eg} = \frac{g_{22}}{|y_{21}|^2}. \tag{10}$$

It should be noticed that (9) is quite similar to the expression for noise figure given in (1). This suggests that a graphical representation similar to that for the noise figure can be expected for the available power gain.

C. A Graphical Representation of Available Power Gain on the Rectangular Source Admittance Plane

Rearranging (9), the following equation can be derived:

$$(G_s - G_G)^2 + (B_s - B_G)^2 = G_{RG}^2 \tag{11}$$

where

$$G_G = G_{og} + \frac{1}{2R_{eg}}\left(\frac{1}{G_a} - \frac{1}{G_{a_{max}}}\right) \tag{12}$$

$$B_G = B_{og} \tag{13}$$

$$G_{RG} = \left[\frac{G_{og}}{R_{eg}}\left(\frac{1}{G_a} - \frac{1}{G_{a_{max}}}\right) + \frac{1}{4R_{eg}^2}\left(\frac{1}{G_a} - \frac{1}{G_{a_{max}}}\right)^2\right]^{1/2}. \tag{14}$$

Equation (11) represents a family of circles on the rectangular coordinates with G_s as the abscissa and B_s as the ordinate, as shown in Fig. 2. Each circle represents a constant G_a locus and has its center at the point (G_G, B_G) and a radius of G_{RG}. G_G and G_{RG} depend upon the value of G_a, but B_G is independent of G_a. Therefore, the locus of the center points for constant G_a becomes a straight line parallel to and at a distance of B_{og} from the abscissa.

III. Noise Measure

A. An Expression for the Noise Measure in Terms of Two-port Parameters and Source Admittance

Substituting (1) and (9) into (2), the noise measure can be expressed in terms of the gain parameters, noise parameters, and source admittance as follows.

$$M = \frac{F_{min} - 1 + \frac{R_{ef}}{G_s}[(G_s - G_{of})^2 + (B_s - B_{of})^2]}{1 - \frac{1}{G_{a_{max}}} - \frac{R_{eg}}{G_s}[(G_s - G_{og})^2 + (B_s - B_{og})^2]}. \tag{15}$$

Rearranging (15), the following equation can be derived,

$$(G_s - G_M)^2 + (B_s - B_M)^2 = G_{RM}^2 \tag{16}$$

where

$$G_M = \frac{M\left(2R_{eg}G_{og} - \frac{1}{G_{a_{max}}} + 1\right) + 2R_{ef}G_{of} - F_{min} + 1}{2(MR_{eg} + R_{ef})} \tag{17}$$

$$B_M = \frac{MR_{eg}B_{og} + B_{of}R_{ef}}{MR_{eg} + R_{ef}} \tag{18}$$

$$G_{RM} = \frac{1}{2(MR_{eg} + R_{ef})}\left[\left\{M\left(\frac{1}{G_{a_{max}}} - 1\right) + F_{min} - 1\right\}^2 - 4(MR_{eg}G_{og} + R_{ef}G_{of})\left\{M\left(\frac{1}{G_{a_{max}}} - 1\right) + F_{min} - 1\right\} - 4MR_{eg}R_{ef}(|Y_{og}|^2 + |Y_{of}|^2 - 4B_{og}B_{of})\right]. \tag{19}$$

For the condition

$$G_{RM} = 0, \tag{20}$$

M takes on its minimum value M_{min}, i.e.,

$$M_{min} = \frac{M_2}{M_1}\left[1 + \left(1 - \frac{M_1M_3}{M_2^2}\right)^{1/2}\right] \tag{21}$$

where

$$M_1 = \left(1 - \frac{1}{G_{a_{max}}}\right)^2 + 4\left(1 - \frac{1}{G_{a_{max}}}\right)R_{eg}G_{og} \tag{22}$$

$$M_2 = \left(1 - \frac{1}{G_{a_{max}}} + 2R_{eg}G_{og}\right)(F_{min} - 1 - 2R_{ef}G_{of}) - 2R_{eg}R_{ef}(|Y_{og}|^2 + |Y_{of}|^2 - 2B_{og}B_{of}) \tag{23}$$

$$M_3 = (F_{min} - 1)^2 - 4(F_{min} - 1)R_{ef}G_{of}. \tag{24}$$

The source conductance and susceptance which produce the minimum noise measure are

$$G_{om} = \frac{M_{min}\left(2R_{eg}G_{og} - \frac{1}{G_{a_{max}}} + 1\right) + 2R_{ef}G_{fo} - F_{min} + 1}{2(M_{min}R_{eg} + R_{ef})} \tag{25}$$

$$B_{om} = \frac{M_{min}R_{eg}B_{og} + R_{ef}B_{of}}{M_{min}R_{eg} + R_{ef}}. \tag{26}$$

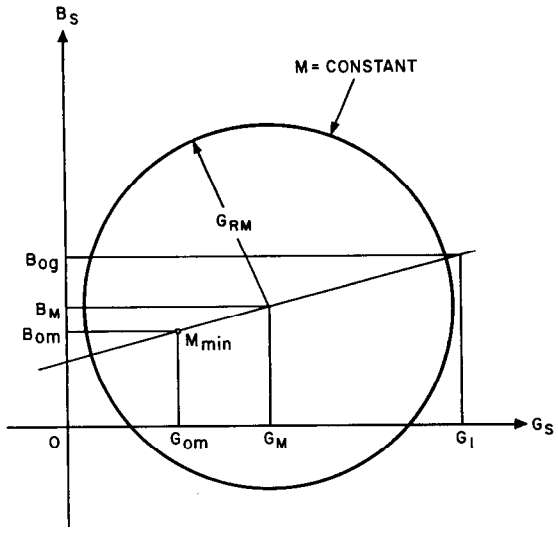

Fig. 3. Constant noise measure locus on rectangular source admittance plane.

B. A Graphical Representation of Noise Measure on the Rectangular Source Admittance Plane

Equation (16) represents a family of circles on the rectangular coordinates with G_s as the abscissa and B_s as the ordinate as shown in Fig. 3. Each circle gives a constant M locus and has its center at the point (G_M, B_M) and a radius of G_{RM}. Since G_M, B_M, and G_{RM} are functions of M, the locus of the center points (G_M, B_M) is not parallel to the abscissa. However, this locus is still given by a straight line through points (G_{om}, B_{om}) and (G_∞, B_{og}), corresponding to unity G_a.

IV. Bilinear Transformations of the Graphical Representations

Equations (11) and (16) and a corresponding equation for the noise figure can be rewritten in a form more convenient for representing the behavior of G_a, F, and M on the complex reflection coefficient plane [6], defined as

$$\rho = u + jv = |\rho| \exp(-j\varphi) = \frac{1 - y_s}{1 + y_s} \tag{27}$$

where

$$y_s = g_s + jb_s = \frac{1}{Y_0}(G_s + jB_s) \tag{28}$$

and Y_0 is the (real) characteristic admittance of the input transmission line. A merit of this plane is that a half-plane with either positive or negative conductance can be represented entirely within a unit circle.

Since ρ is a bilinear function of the complex number y_s, any circule in the Y_s-plane can be transformed into a circle in the ρ-plane. Thus, (11) and (16) and the corresponding equation for the noise figure can be expressed in the form

$$(u - u_i)^2 + (v - v_i)^2 = r_i^2 \tag{29}$$

where the subscript j represents g, f, and m for G_a, F, and M, respectively. (u_j, v_j) and r_j, respectively, give the coordinate points for the center of a constant G_a (or F, M) circle and its radius. The center point is also given by the polar coordinates, $|\rho|$ and φ, in the ρ-plane. Furthermore, the Smith-chart coordinates, g_s and b_s, are related to the rectangular coordinates in the manner [7],

$$g_s = \frac{1 - u^2 - v^2}{(1 + u)^2 + v^2} \tag{30}$$

$$b_s = \frac{-2v}{(1 + u)^2 + v^2}. \tag{31}$$

Therefore, the center point can also be specified in terms of g_s and b_s in the same ρ-plane.

Since φ is constant for all constant G_a and F loci as seen later, the polar coordinates is most convenient for mapping G_a and F in the ρ-plane. On the other hand, φ depends upon M so that a preferable coordinate is no longer offered for drawing constant M loci.

In the polar ρ-plane the center point and the radius of a constant G_a circle are given as follows:

$$|\rho_g| = \frac{[(1 - g_{og}^2 - b_{og}^2)^2 + 4b_{og}^2]^{1/2}}{(1 + g_{og})^2 + b_{og}^2 + 2\delta_g} \tag{32}$$

$$\varphi_g = \tan^{-1}\left[\frac{2b_{og}}{1 - g_{og}^2 - b_{og}^2}\right] \tag{33}$$

$$r_g = \frac{2g_{RG}}{(1 + g_{og})^2 + b_{og}^2 + 2\delta_g} \tag{34}$$

where

$$\delta_g = \frac{1}{2R_{eg}Y_0}\left(\frac{1}{G_a} - \frac{1}{G_{amax}}\right) \tag{35}$$

and g_{og}, b_{og}, and g_{RG} are normalized values of G_{og}, B_{og}, and G_{RG} with respect to Y_0. The radial coordinate $|\rho_{og}|$ for G_{amax} is then given by taking δ_g equal to zero. Figure 4 illustrates the geometrical relations of the above parameters in the ρ-plane.

For the noise figure, completely identical forms to the above are available simply by replacing the subscripts. In this case δ_f should be

$$\delta_f = \frac{F - F_{min}}{2R_{ef}Y_0}. \tag{36}$$

If the Smith-chart coordinates are employed for the mapping of the noise measure, the center point and the radius of a constant M circle are given by

$$g_m = \frac{(1 + g_M)[(1 + g_M)g_M + b_M^2 - g_{RM}^2] - b_M^2}{(1 + g_M)^2 + b_M^2} \tag{37}$$

$$b_m = \frac{b_M[(1 + g_M)^2 + b_M^2 - g_{RM}^2]}{(1 + g_M)^2 + b_M^2} \tag{38}$$

$$r_m = \frac{g_{RM}}{(1 + g_M)^2 + b_M^2 - g_{RM}^2} \tag{39}$$

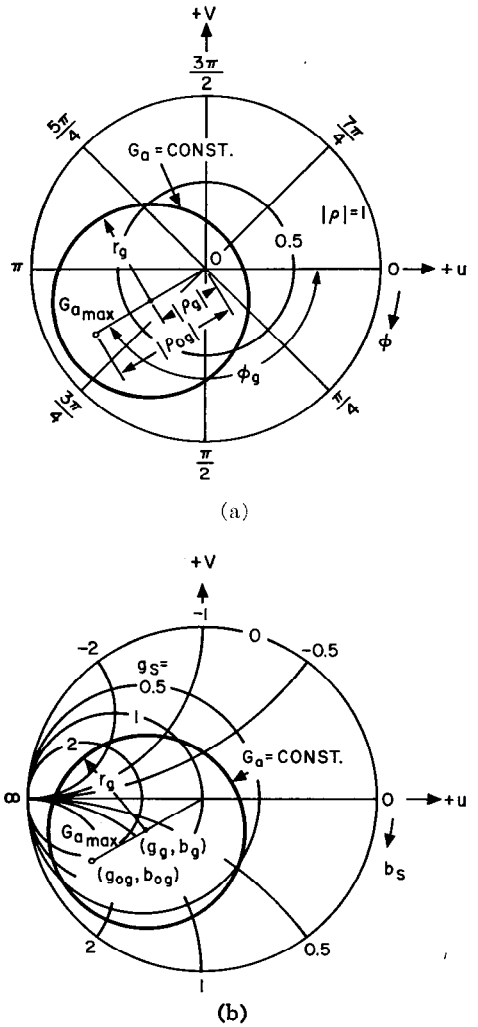

Fig. 4. (a) Constant available power gain locus on complex reflection coefficient plane. (b) Constant available power gain locus on the Smith-chart.

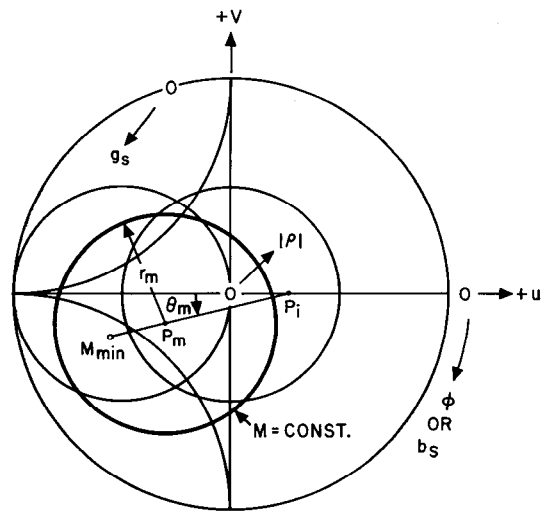

M_{min}: $(|\rho_{om}|, \phi_{om})$ OR (g_{om}, b_{om})
P_i: $(|u_i|, 0)$ OR $(g_i, 0)$
P_m: $(|\rho_m|, \phi_m)$ OR (g_m, b_m)

Fig. 5. Constant noise measure locus on the Smith-chart.

where again small letters indicate normalized values of capital letters with respect to Y_0. The coordinates for M_{min} are, of course, designated by g_{om} and b_{om}.

Due to the nature of the bilinear transformation, the locus connecting the centers of the constant-M circles is still a straight line on the ρ-plane. Its angle θ_m and intersecting point g_i with the abscissa are given by

$$\tan\theta_m = \left[\left\{F_{min} - 1 - R_{ef}Y_0\left(\frac{|Y_{of}|^2}{Y_0^2} + \frac{2G_{of}}{Y_0} + 1\right)\right\}R_{eg}B_{og} - \left\{\frac{1}{G_{amax}} - 1 - R_{eg}Y_0\left(\frac{|Y_{og}|^2}{Y_0^2} + \frac{2G_{og}}{Y_0} + 1\right)\right\}R_{ef}B_{of}\right] \cdot \left[(F_{min} - 1)\left(\frac{|Y_{og}|^2}{Y_0^2} - 1\right)\frac{R_{eg}Y_0}{2} - \left(\frac{1}{G_{amax}} - 1\right) \cdot \left(\frac{|Y_{of}|^2}{Y_0^2} - 1\right)\frac{R_{ef}Y_0}{2} + \left\{|Y_{of}|^2\left(\frac{G_{og}}{Y_0} + 1\right) - |Y_{og}|^2\left(\frac{G_{of}}{Y_0} + 1\right) + Y_0(G_{of} - G_{og})\right\}R_{eg}R_{ef}\right]^{-1} \quad (40)$$

$$g_i = \frac{(1 + g_{om})g_{om} - (\cot\theta_m - b_{om})b_{om}}{1 + g_{om} + b_{om}\cot\theta_m}. \quad (41)$$

θ_m can be determined only by the gain and the noise parameters and is independent of M as seen in (40). For the mapping of constant M circles, the center points can also be given by this line and either g_m or b_m, instead of g_m and b_m. In practice, this line is simply drawn by connecting two representative points, (g_{om}, b_{om}) and (g_i, b_{og}), corresponding to unity G_a. Figure 5 shows the mapping of constant M locus on the Smith-chart where the polar reflection coefficient coordinates also overlap.

V. Exchangeable Power Gain, Extended Noise Figure, and Extended Noise Measure

The noise figure is normally defined in terms of available power gain as given in (1). However, the available power concept leads to difficulties when the input and output admittances of two-ports have negative real parts. Such cases can, in general, be handled in a similar manner by using the exchangeable power and gain concepts in place of available power and gain. This leads to an extended definition of the noise figure [8]. Using the exchangeable power gain G_e and the extended noise figure F_e, an extended noise measure M_e can be defined as [3]

$$M_e = \frac{F_e - 1}{1 - \frac{1}{G_e}}. \quad (42)$$

In the above cases, the graphical representations of G_e, F_e, and M_e on the source admittance planes are also available in similar ways. In some cases, minor modifications will be required, for example, use of a negative conductance Smith-chart [9], an expanded Smith-chart outside the unit circle to include both positive and negative conductances, and so on.

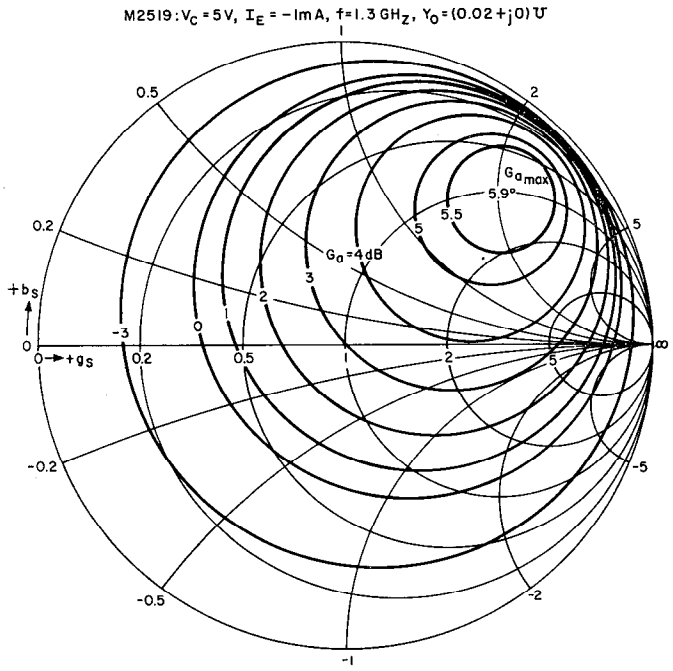

Fig. 6. Available power gain chart.

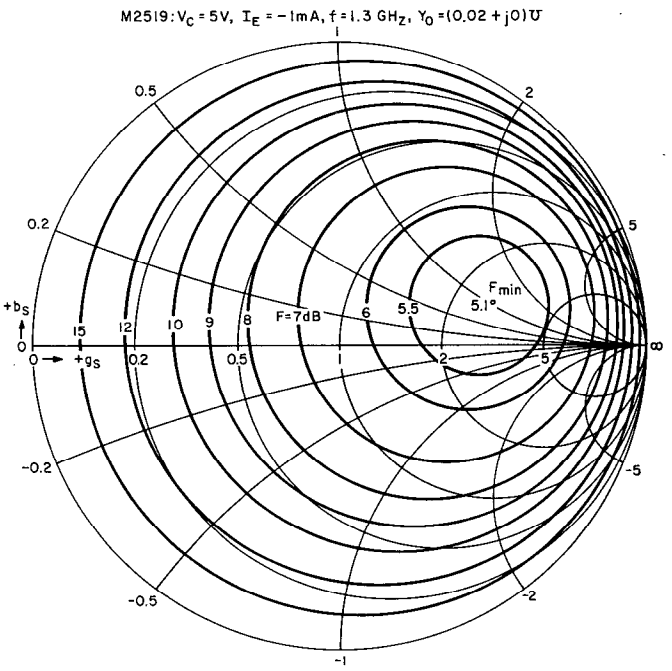

Fig. 7. Noise figure chart.

VI. Examples of Graphical Representations

A. Device Characteristics

A silicon *n-p-n* double-diffused planar microwave transistor M2519 was used in actual representations of available power gain, noise figure, and noise measure of its equivalent two-port. This transistor was characterized at an emitter current of −1 mA, collector voltage of 5 volts, and frequency of 1.3 GHz. The measurements of the gain and the noise parameters were made using the method recommended by the IRE Standard Committee on Electron Tubes [1], [10]. The gain parameters can also be determined by a rather simple method in which $G_{a_{max}}$, G_{og}, and B_{og} are directly obtained. Using the relation of (12), R_{eg} can then be determined by the aid of another measurement of the available power gain with a given source admittance, for example, $Y_s = (0.02 + j0)$ mho. Another way for determining the gain parameters is to use the measured y-parameters (or any suitable two-port parameters) as seen in (5) through (8) and (10).

Predetermined parameter values are as follows:

$G_{a_{max}} = 3.93(5.9\text{ dB})$
$R_{eg} = 2.54$ ohms
$G_{og} = 18.4$ millimhos
$B_{og} = 44.2$ millimhos
$F_{min} = 3.25(5.1\text{ dB})$
$R_{ef} = 15.6$ ohms
$G_{of} = 53$ millimhos
$B_{of} = 20$ millimhos

From the above parameters, the following parameters were obtained:

$M_{min} = 3.32\ (5.2\text{ dB})$
$G_{om} = 47$ millimhos
$B_{om} = 30$ millimhos.

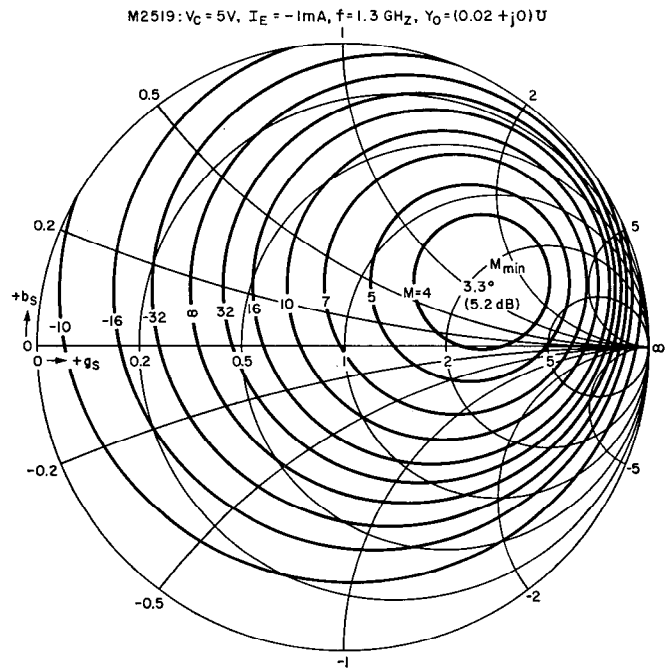

Fig. 8. Noise measure chart.

B. Graphical Representations on the Smith-Chart

The available power gain, noise figure, and noise measure for the same transistor are shown on a Smith-chart representation of source admittance, as shown in Figs. 6, 7, and 8, respectively. From these figures, it can be understood easily and precisely what source admittance is able to give a good performance for the amplifier and how the situation becomes worse as the source admittance differs from the optimum value.

As expected, the locus for infinite M coincides with

that for unity G_a and the coordinate point for M_{min} is located between those for $G_{a_{max}}$ and F_{min}.

VII. Conclusions

In this paper it has been shown that the noise measure of linear two-ports can be expressed in terms of the gain parameters, the noise parameters, and the source admittance. Constant M loci have been represented in the source admittance plane as well as constant G_a and constant F loci. Transformations of these loci into the Smith-chart have been made, since this is a very convenient way of representing a wide range of immittances. Such a mapping is useful when the gain and noise performance of amplifiers is investigated, especially in the microwave region. By looking at the noise measure chart, for example, it is easy to deduce what source admittance gives the best overall noise performance and how it deteriorates as the admittance differs from its optimum value. These effects were demonstrated using a microwave transistor as an example.

References

[1] "IRE Standards on Electron Tubes: Methods of Testing," 1962, 62 IRE 7 S1, pt. 9: "Noise in linear twoports."

[2] H. Rothe and W. Dahlke, "Theory of noisy fourpoles," *Proc. IRE*, vol. 44, pp. 811–818, June 1956.

[3] H. A. Haus and R. B. Adler, *Circuit Theory of Linear Noisy Networks*. New York: Wiley, 1959.

[4] ——, "Invariants of linear noisy networks," *1956 IRE Conv. Rec.*, pt. 2, pp. 53–67, 1956.

[5] J. G. Linvill and J. F. Gibbons, *Transistors and Active Circuits*, New York: McGraw-Hill, 1961. The authors gave a wrong expression for available power gain in their book, probably due to typographical errors.

[6] J. C. Slater, "Microwave Electronics," *Rev. Mod. Phys.*, vol. 18, pp. 441–512, October 1946.

[7] P. H. Smith, "Transmission-line calculator," *Electronics*, vol. 12, pp. 29–31, January 1939; and "An improved transmission-line calculator," *Electronics*, vol. 17, p. 130, January 1944.

[8] H. A. Haus and R. B. Adler, "An extension of the noise figure definition," *Proc. IRE (Correspondence)*, vol. 45, pp. 690–691, May 1957.

[9] H. Fukui, "The characteristics of Esaki diodes at microwave frequencies," *1961 ISSCC Digest of Tech. Papers*, pp. 16–17, 1961; and *J. IECE (Japan)*, vol. 43, pp. 1351–1356, November 1960 (in Japanese).

[10] ——, "The noise performance of microwave transistors," *IEEE Trans. on Electron Devices*, vol. ED-13, pp. 329–341, March 1966.

A Simple and Efficient Algorithm for Determining Isomorphism of Planar Triply Connected Graphs

LOUIS WEINBERG, FELLOW, IEEE

Abstract—**A problem that arises in many practical applications of linear graphs and in some purely mathematical applications is the determination of the isomorphism of two given graphs; such applications include the automatic retrieval of information, machine translation of languages, pipeline and electric networks, pattern recognition, graph-theoretic enumeration problems, the four-color conjecture, and the problem of "squaring the rectangle." Up to the present time only heuristic programs have been developed for solving this problem for general graphs. In this paper, a solution for a class of graphs is given in terms of a simple and computationally efficient algorithm, which is ideally suited for computer programming; a program in MAD language has been written but has not yet been run. The class of graphs considered are planar and triply connected; this class arises, for example, in the four-color problem and in the problem of squaring the rectangle. The algorithm is applicable to both directed and undirected graphs and to simple graphs and multigraphs. The algorithm is based on Trémaux's procedure for generating an Euler path in a graph. Application of the algorithm to a plane triply connected graph yields a set of vector codes which are ordered lexicographically in a code matrix. Two isomorphism theorems are then stated and proved; one theorem asserts that two-plane triply connected graphs are isomorphic if and only if their code matrices are equal. Finally, two significant examples are used as illustrations of how the basic procedure may be shortened by combining it with a check on some simple necessary conditions so that it becomes almost computationally trivial, that is, large graphs can be tested quickly "by hand."**

Manuscript received August 17, 1965; revised February 17, 1966. This research was jointly supported by the Radar Laboratory under Project Michigan, Department of the Army, Contract DA 28-043-AMC-00013(E), and by the Institute of Science and Technology, University of Michigan, Ann Arbor, Mich.

The author is with the Department of Electrical Engineering, City College of City University of New York, N. Y. He was formerly with the Department of Electrical Engineering and The Institute of Science and Technology, University of Michigan.

I. Introduction

IN THIS PAPER we solve a problem that arises in many practical and theoretical applications of linear graphs. Familiar practical applications are electrical or pipeline networks; less familiar ones are computer programs and computer storage-allocation schemes. Some recent work on pattern recognition has also used linear graphs, where given patterns are matched with previously available classified patterns. For example, the pattern for a chemical molecule may be compared with a dictionary of patterns of molecules; patterns of language structure are represented by trees so that syntactic analysis and automatic translation of languages may be carried out; finally, in document retrieval and the automatic retrieval of information, a linear graph representation of the desired information is compared with the linear graphs